Neurite Orientation Dispersion and Density Imaging for Assessing Acute Inflammation and Lesion Evolution in MS

S. Sacco, E. Caverzasi, N. Papinutto, C. Cordano, A. Bischof, T. Gundel, S. Cheng, C. Asteggiano, G. Kirkish, J. Mallott, W.A. Stern, S. Bastianello, R.M. Bove, J.M. Gelfand, D.S. Goodin, A.J. Green, E. Waubant, M.R. Wilson, S.S. Zamvil, B.A. Cree, S.L. Hauser, R.G. Henry, and and University of California, San Francisco MS-EPIC Team

AJNR Am J Neuroradiol 2020, 41 (12) 2219-2226
doi: https://doi.org/10.3174/ajnr.A6862
http://www.ajnr.org/content/41/12/2219

Neurite Orientation Dispersion and Density Imaging for Assessing Acute Inflammation and Lesion Evolution in MS

S. Sacco, E. Caverzasi, N. Papinutto, C. Cordano, A. Bischof, T. Gundel, S. Cheng, C. Asteggiano, G. Kirkish, J. Mallott, W.A. Stern, S. Bastianello, R.M. Bove, J.M. Gelfand, D.S. Goodin, A.J. Green, E. Waubant, M.R. Wilson, S.S. Zamvil, B.A. Cree, S.L. Hauser, R.G. Henry, and University of California, San Francisco MS-EPIC Team

ABSTRACT

BACKGROUND AND PURPOSE: MR imaging is essential for MS diagnosis and management, yet it has limitations in assessing axonal damage and remyelination. Gadolinium-based contrast agents add value by pinpointing acute inflammation and blood-brain barrier leakage, but with drawbacks in safety and cost. Neurite orientation dispersion and density imaging (NODDI) assesses microstructural features of neurites contributing to diffusion imaging signals. This approach may resolve the components of MS pathology, overcoming conventional MR imaging limitations.

MATERIALS AND METHODS: Twenty-one subjects with MS underwent serial enhanced MRIs (12.6 ± 9 months apart) including NODDI, whose key metrics are the neurite density and orientation dispersion index. Twenty-one age- and sex-matched healthy controls underwent unenhanced MR imaging with the same protocol. Fifty-eight gadolinium-enhancing and non-gadolinium-enhancing lesions were semiautomatically segmented at baseline and follow-up. Normal-appearing WM masks were generated by subtracting lesions and dirty-appearing WM from the whole WM.

RESULTS: The orientation dispersion index was higher in gadolinium-enhancing compared with non-gadolinium-enhancing lesions; logistic regression indicated discrimination, with an area under the curve of 0.73. At follow-up, in the 58 previously enhancing lesions, we identified 2 subgroups based on the neurite density index change across time: Type 1 lesions showed increased neurite density values, whereas type 2 lesions showed decreased values. Type 1 lesions showed greater reduction in size with time compared with type 2 lesions.

CONCLUSIONS: NODDI is a promising tool with the potential to detect acute MS inflammation. The observed heterogeneity among lesions may correspond to gradients in severity and clinical recovery after the acute phase.

ABBREVIATIONS: AD = axial diffusivity; DAWM = dirty-appearing white matter; FA = fractional anisotropy; FU = follow-up; GEL = gadolinium-enhancing lesion; HC = healthy control; MD = mean diffusivity; NAWM = normal-appearing white matter; NDI = neurite density index; NGEL = non-gadolinium-enhancing lesion; NODDI = neurite orientation dispersion and density Imaging; nODI = normalized orientation dispersion index; ODI = orientation dispersion index; RD = radial diffusivity; VEC = extra-neurite compartment

Conventional MR imaging is essential for MS diagnosis and management, specifically for demonstrating WM lesion dissemination in space (involvement of >1 CNS region) and time (across time accumulation).[1] Conventional MR imaging, however, lacks specificity in characterizing MS WM lesions after the acute phase; all lesions show a similar radiologic appearance on T2WI, irrespective of the degree of inflammation, axonal loss, gliosis,

Received May 4, 2020; accepted after revision July 29.

From the Department of Neurology (S.S., E.C., N.P., C.C., A.B., T.G., S.C., C.A., G.K., J.M., W.A.S., R.M.B., J.M.G., D.S.G., A.J.G., E.W., M.R.W., S.S.Z, B.A.C., S.L.H., and R.G. H.), University of California, San Francisco Weill Institute for Neurosciences, University of California, San Francisco, California; Institute of Radiology (S.S., C.A.), Department of Clinical Surgical Diagnostic and Pediatric Sciences, and Department of Brain and Behavioral Sciences (S.B.), University of Pavia, Pavia, Italy; and Neuroradiology Department (S.B.), Istituto Di Ricovero e Cura a Carattere Scientifico Mondino Foundation, Pavia, Italy.

This work was supported by a gift from the Ostby Foundation (R.G.H.); the National Institute of Neurological Diseases and Stroke (R35NS111644, S.L.H.; RO1NS26799,. S.L.H.; K23 NS048869, B.A.C.); the National MS Society (RG-1707-28775, R.G.H.); the Valhalla Foundation; and gifts from Friends of the Multiple Sclerosis Research Group at UCSF.

Paper previously presented at: 56th annual meeting of the ASNR (American society of Neuroradiology), June 2–7, 2018, Vancouver, Canada; NAIMS, North American Imaging in Multiple Sclerosis Cooperative workshop meeting, February 27, 2019, Dallas; ACTRIMS, Annual americas committee for treatment and research in multiple sclerosis Forum, February 28–March 2, 2019, Dallas; and Annual Meeting of the International Society of Magnetic Resonance in Medicine, May 11–16, 2019, Montreal, Quebec, Canada.

Please address correspondence to Simone Sacco, MD, Department of Neurology, UCSF Weill Institute for Neurosciences, University of California San Francisco, 675 Nelson Rising Ln, San Francisco, CA 94158; e-mail: saccosimone88@gmail.com

Indicates open access to non-subscribers at www.ajnr.org
Indicates article with supplemental online appendix and table.
Indicates article with supplemental online photo.
http://dx.doi.org/10.3174/ajnr.A6862

demyelination, and remyelination.[2,3] Furthermore, clinical disability shows limited correlation with volume and the number of detectable WM lesions. The different neuropathologic characteristics of WM lesions as well as the accumulation of tissue damage within normal-appearing WM (NAWM) are some of the other factors possibly playing a role in the development of MS disability.[4]

Gadolinium-based imaging improves the utility of conventional MR imaging in MS because gadolinium-enhancing lesions (GELs) represent a radiologic correlate of acute inflammation, corresponding to active lesions associated with blood-brain barrier disruption. However, despite its importance for diagnosis (fulfillment of dissemination in time criteria), the application of gadolinium-based contrast agents has raised a number of safety concerns.[5] Therefore, alternative MR imaging markers of acute inflammation are needed.

Neurite orientation dispersion and density imaging (NODDI) is a clinically feasible diffusion MR imaging technique, incorporating multiple shells with different b-values to model brain tissue into 3 compartments showing different diffusion properties.[6] According to this orientation-dispersed cylindric model, the isotropic diffusion fraction is highly represented only within CSF, whereas within brain parenchyma, the diffusion signal can be either hindered (Gaussian displacement pattern) or restricted (non-Gaussian displacement pattern). The hindered signal is attributed to the extraneurite compartment (VEC), defining the extracellular volume fraction whereas the restricted signal is attributed to intraneurite spaces and is thought to correspond to the neurite density index (NDI). A Watson distribution is then used to compute the orientation distribution of the cylinders, quantified from 0 to 1 by the orientation dispersion index (ODI). Highly compacted and parallel WM bundles, such as the corpus callosum, generally show lower ODI values compared with the cortical and subcortical regions, characterized by multidirectional dendritic structures.

Even though NODDI applications are novel in MS, this technique appears promising in detecting and modeling the complexity of MS pathology, being potentially more specific than DTI in capturing microstructural substrates.[7-12] NODDI has never been used, however, to assess longitudinal changes within MS lesions and NAWM. For animal studies, only a single work, based on a murine model, longitudinally assessed induced demyelinated lesions, correlating NODDI abnormalities with histopathologic changes.[13] The authors suggested that after a demyelinating event, the combination of decreasing ODI and increasing NDI with time might reflect improvement in fiber coherency due to remyelination.

The aim of this work was to cross-sectionally assess the role of NODDI in indicating gadolinium enhancement in acute lesions and to longitudinally assess NODDI and conventional DTI changes in MS lesions and NAWM in the transition from detectable to undetectable gadolinium enhancement. We hypothesized that NODDI-derived metrics may be promising markers to detect acute inflammation as well as heterogeneity among lesions and their evolution with time.

MATERIALS AND METHODS

Subjects

A subgroup of subjects with MS participating in the UCSF EPIC study[14,15] was identified on the basis of the following inclusion criteria: 1) confirmed MS or clinically isolated syndrome diagnosis; 2) at least 2 longitudinal 3T MR imaging scans during 2 years, including a NODDI multishell dedicated protocol of adequate quality; 3) the presence of at least 1 enhancing lesion at baseline that had to be resolved at the follow-up examination; and 4) absence of new enhancing lesions at follow-up. The Committee on Human Research at our institution (UCSF) approved the study protocol. Written informed consent was obtained from all participants.

Of 290 subjects assessed from 2015 to 2018, 21 met the study entry requirements (mean age, 36.4 ± 8.7 years, 17 women). Sixteen of them had relapsing-remitting MS, 3 had clinically isolated syndrome, and 2 had primary-progressive MS with an average Expanded Disability Status Scale score of 2.6+ ± 1.6. For each subject, we chose as follow-up MRI (12.6 ± 9 months apart) the first MRI showing complete resolution of enhancement and absence of new enhancing lesions.

We studied 21 age- and sex-matched healthy controls (HCs) (mean age, 36.4 ± 8.7 years; 17 women).

MRI Protocol

Subjects underwent longitudinal (2 or 3 time points) 3T MRIs (Magnetom Skyra; Siemens) with a high-angular-resolution diffusion imaging 2-shell acquisition protocol (simultaneous multisection sequence, section acceleration factor of two, 30 directions at $b = 700$ s/mm^2, and 64 directions at $b = 2000$ s/mm^2 with TR/TE = 4300/96 ms, along with 10 $b = 0$ scans, 1 of which was acquired using a reversed phase-encoding direction, posterior to anterior; 2.2-mm^3 isotropic voxels; 66 axial slices; FOV = 220 × 220 mm). The NODDI protocol was added to the conventional MR imaging sequences (pre- and postcontrast 3D T1WI 1-mm^3 cubic voxel MPRAGE and FLAIR) performed at each visit. HCs underwent 1 unenhanced 3T MR imaging with the same protocol.

NODDI and DTI Processing and Imaging Coregistration

First, susceptibility-induced distortions were estimated from image pairs acquired with reversed phase-encoding directions (resulting in distortions with opposite directions), analogous to Andersson et al,[16] using the "TOPUP" tool of the FMRIB Software Library (FSL; http://fsl.fmrib.ox.ac.uk/fsl/fslwiki/topup).[17] Additionally, eddy current–induced distortions and head motion were estimated and corrected using "eddy" from the same toolbox (https://fsl.fmrib.ox.ac.uk/fsl/fslwiki/eddy); b-vectors were accordingly rotated to account for the corrections.

NODDI fitting was performed with the NODDI Matlab Toolbox (Version1.0.1; MathWorks) and DTI using DIPY, Version 0.13.[18] To analyze the NODDI and DTI metrics within the same ROIs for both time points, we performed a linear registration using FMRIB's Linear Image Registration Tool (FLIRT; http://www.fmrib.ox.ac.uk/fsl/fslwiki/FLIRT) for aligning the T1WI MPRAGE, FLAIR, and postgadolinium T1WI MPRAGE images to their baseline time point. For each time point and for the HC scans, the Anisotropic Power Map derived from the high-angular-resolution diffusion imaging data was then registered to the T1WI MPRAGE images using the ANTS (http://stnava.github.io/ANTs/) multidimensional registration tool. The same transformation used to register the Anisotropic Power Map was then applied to each of the

NODDI and DTI maps to register the images into the same space. Visual quality checks of the registration results were performed.

Selection of ROIs in Subjects with MS

Acute Lesions: GELs. Acute lesions were studied longitudinally at both baseline and follow-up.

Specifically, at baseline S.S. semiautomatically segmented 140 GELs on 21 subjects using Jim (http://www.xinapse.com/home.php) on postgadolinium T1WI. The results were reviewed by E.C., and consensus was eventually achieved. The ROIs were subsequently checked on the baseline FLAIR and manually edited to include any voxel of abnormal FLAIR hyperintensity. We used these modified GEL ROIs for analysis. Each lesion in each subject was indexed.

Starting from GEL baseline masks, we created GEL follow-up masks (GEL-FU) by manually modifying the ROIs on the follow-up FLAIR. The manual editing was performed to take into account the evolution in size of a lesion after enhancement resolution to avoid inclusion of contiguous NAWM within GEL-FU ROIs. All GEL-FU lesions were nonenhancing.

NODDI data were registered to the T1-weighted image that had a higher resolution. Only lesions that had at least twenty-five 1-mm^3 voxels at both baseline and follow-up were included to avoid inaccuracies due to partial volume effects.

Chronic Lesions: Non-Gadolinium-Enhancing Lesions. Chronic lesions were studied longitudinally at both baseline and follow-up.

For comparison, we selected 58 nonenhancing lesions, >25 voxels from the same subjects who showed the GELs used in our final analysis. We refer to this last mask as non-gadolinium-enhancing lesions (NGELs). NGEL follow-up masks (NGEL-FU) were created with manual edits as described above. Each lesion in each subject was indexed.

Normal-Appearing White Matter and Dirty-Appearing White Matter. An in-house-developed algorithm was applied to delineate dirty-appearing white mater (DAWM). DAWM was defined as having a T2-weighted signal intensity intermediate between lesions and NAWM.[19] The first step of this algorithm uses FSL SIENAX (http://fsl.fmrib.ox.ac.uk/fsl/fslwiki/SIENA)[20] to segment WM and cortical GM as well as FreeSurfer (http://surfer.nmr.mgh.harvard.edu) to segment subcortical GM. FMRIB's Integrated Registration and Segmentation Tool (FIRST; http://fsl.fmrib.ox.ac.uk/fsl/fslwiki/FIRST) was then used within the boundaries of the WM mask created from the steps above to separate the WM into 2 tissue types: NAWM and DAWM. E.C. and S.S. reviewed the DAWM probability maps and chose a 0.95 threshold to obtain a final DAWM ROI. The final NAWM masks were generated by subtracting lesions, DAWM masks, subcortical GM, and infratentorial regions from SIENAX WM masks.

Extraction of NODDI and DTI Metrics from NAWM, DAWM, GELs, GEL-FU, NGELs, and NGEL-FU

Median values of ODI, NDI, and DTI metrics were extracted within GELs at the time of enhancement and GEL-FU after resolution of enhancement. Median values of ODI, NDI, and DTI metrics were extracted at both time points within the NAWM and DAWM masks. As values of reference for chronic lesions, we extracted ODI, NDI, and DTI metrics from NGEL masks at baseline and NGEL-FU masks at follow-up.

For ODI values, an upper threshold of 0.5 was used to minimize potential partial volume effects with CSF and GM. Isotropic volume fraction differences between lesions and NAWM, DAWM, and healthy control WM (HCWM) were too small to be estimated. The fraction of water able to move isotopically within brain WM is indeed generally low. To potentially account for isotropic volume fraction variation, however, we corrected NDI and VEC values, dividing them for the global amount of anisotropic diffusion (VEC + NDI). In this context, VEC and NDI become exactly specular within each voxel of the brain; therefore, in the current study, we only report NDI values to avoid redundant information.

Healthy Control WM Values

HC MRIs were used to furnish NODDI and DTI WM values of reference in the healthy control population as described in the Online Appendix.

Statistical Analysis

To compare values across different brain regions, we normalized ODI values (nODI) by computing the percentage change from HC values extracted as described in the Online Appendix (ie, the subject's ODI/HC ODI in the same ROI).

We used a 2-sided *t* test to assess differences in NODDI and DTI metrics among GELs, NGELs, NAWM, DAWM, and HCWM. Longitudinal differences in NODDI and DTI metrics within NAWM, DAWM, GEL, and NGEL masks were assessed using a 2-sided paired *t* test.

Logistic regression analysis was performed using nODI to calculate the NODDI power to discriminate GELs from NGELs at baseline as well as the gadolinium-enhancing phase (GEL) from a phase without gadolinium enhancement (GEL-FU) within the same lesions.

RESULTS

Subject Treatments

At the baseline scan, 11 subjects were treatment-naïve. Of the 10 treated subjects, 6 had received glucocorticoids 30 days before MR imaging, 3 were on disease-modifying therapies but had not received glucocorticoids, and 1 was on disease-modifying therapies and had received glucocorticoids. At follow-up, 17/21 subjects were on disease-modifying therapies; no subjects received glucocorticoids within 30 days preceding the follow-up scans.

Lesions

Fifty-eight GELs of >25 voxels, distributed among 17 subjects (mean, 3.47 ± 4.35; minimum 1, maximum 18 per subject), were identified and matched to 58 NGELs.

Cross-Sectional Analysis of ODI Values. In the contrast-enhancing phase at baseline, GEL ODI was higher than that in HCWM (0.28 ± 0.07 versus 0.22 ± 0.07; $P < .001$), whereas at follow-up in the nonenhancing phase, GEL-FU ODI had values similar to those in HCWM (0.23 ± 0.08 versus 0.23 ± 0.08; $P = .4$).

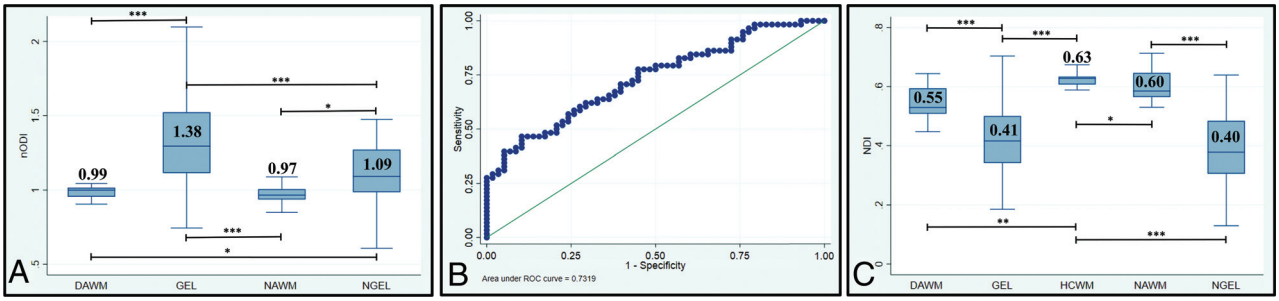

FIG 1. *A*, nODI (ODI pt/ODI HC) values within DAWM, GEL, NAWM, and NGEL masks at baseline with a respective 2-sided *t* test. Only statistically significant differences are reported (*asterisk* = $P < .05$; *2 asterisks* = $P < .005$; *3 asterisks* = $P < .0005$). *B*, Receiver operating characteristic for logistic regression using nODI for discriminating between GELs and NGELs at baseline. *C*, NDI values within DAWM, GELs, HCWM, NAWM, and NGELs at baseline with respective 2-sided t-tests. Only statistically significant differences are reported (*asterisk* = $P < .05$; *2 asterisks* = $P < .005$; *3 asterisks* = $P < .0005$). pt, subject.

Across all subjects, we compared ODI values within different ROIs using nODI to eliminate the influence of location. As shown in Fig 1*A*, baseline nODI was higher in GELs than NGELs (1.38 ± 0.39 versus 1.09 ± 0.22; $P < .001$). Logistic regression indicated that nODI was the best discriminator between GELs and NGELs among NODDI and DTI metrics (the area under curve for nODI is equal to 0.73, whereas the area under curve for fractional anisotropy (FA) is equal to 0.64) (Fig 1*B*).

ODI Change with Time. nODI decreased within GELs from baseline to follow-up (1.38 ± 0.39 versus 1.02 ± 0.24; $P < .001$). nODI decreased even within NGELs from baseline to follow-up (1.09 ± 0.22 versus 1.02 ± 0.26; $P < .05$). Logistic regression indicated that nODI was the best discriminator between GELs and GEL-FU among NODDI and DTI metrics (the area under curve for nODI is equal to 0.83, whereas the area under curve for FA is equal to 0.71).

Cross-Sectional Analysis of NDI Values. As shown in Fig 1*C*, NDI was lower within lesions than in HCWM, NAWM, and DAWM (0.41 ± 0.12 versus 0.63 ± 0.02, 0.60 ± 0.05, 0.55 ± 0.05; $P < .001$). There was no difference in the NDI between GELs and NGELs at baseline (0.42 ± 0.11 versus 0.4 ± 0.14; $P = .4$).

NDI Change with Time, Definition of Lesion Types 1 and 2, and Post Hoc Analyses. On average, there was no NDI change with time within lesions in the transition from the enhancing to nonenhancing phase. However, after resolution of enhancement, 30/58 lesions showed an increased NDI compared with baseline, whereas 28/58 showed a decreased NDI.

In a post hoc analysis, we separated these lesions into 2 groups, lesion type 1 "increasing NDI with time," and lesion type 2, "decreasing NDI with time" using a 2-sided *t* test to look for differences in NODDI and DTI metrics at baseline and follow-up, as well as shrinkage in lesion size, distribution among subjects, and treatment.

During gadolinium enhancement, NDI was lower in lesion type 1 than in lesion type 2 (0.37 ± 0.09 versus 0.47 ± 0.1; $P < .001$), whereas, most interesting, NDI was higher in lesion type 1 than in lesion type 2 following enhancement disappearance (0.48 ± 0.11 versus 0.39 ± 0.11; $P < .005$). Specifically, in lesion type 1, NDI increased with time along with a decrease in ODI, whereas in lesions type 2, NDI decreased with time along with a decrease in ODI (Online Table).

Lesion type 1 showed more pronounced shrinkage compared with lesion type 2 ($P < .05$), decreasing on average by 50% ± 20%, whereas lesion type 2 decreased on average by 38% ± 22% (Online Table).

Of 17 subjects, 8 demonstrated only type 1 lesions, 6 showed both lesion types, and 3 had only type 2 lesions. No statistically significant differences among these groups of subjects were detected regarding glucocorticoid use or disease-modifying therapies before scanning, either at baseline or follow-up.

Differences in DTI Parameters between GELs/GEL-FU and NGELs

NGELs showed lower FA compared with GEL-FU (0.3 ± 0.04 versus 0.37 ± 012; $P < .01$), higher radial diffusivity (RD) compared with GEL-FU (702 ± 84 × 10^{-6} versus 665 ± 14 × 10^{-6}; $P < .005$), higher mean diffusivity (MD) compared with GEL and GEL-FU (840 ± 8 × 10^{-6} versus 790 ± 14 × 10^{-6}, 770 ± 16 × 10^{-6}; $P < .05$), and higher axial diffusivity (AD) compared with GEL (1180 ± 180 versus 1003 ± 240 × 10^{-6}; $P < .005$). The Online Figure shows the comparison of NODDI and DTI metrics between GELs and GEL-FU as well as GELs and NGELs.

Regarding lesion subtypes, type 1 lesions showed decreases with time in MD, RD, and AD and an increase in FA, whereas type 2 lesions showed increases in all the metrics (Online Table).

NAWM and DAWM Changes

ODI. NAWM showed lower ODI compared with HCWM (0.228 ± 0.0002 versus 0.234 ± 0.0001; $P < .05$) at both baseline and follow-up. No difference was detected between HCWM and DAWM ODI at both baseline and follow-up. At baseline, nODI was lower in NAWM and DAWM compared with both GELs and NGELs (0.97 ± 0.06, 0.99 ± 0.07 versus 1.38 ± 0.39, 1.09 ± 0.22; $P < .05$) (Fig 1*A*), whereas at follow-up, no difference was detectable.

Differences in nODI between NAWM and DAWM were not significant at baseline or follow-up.

There was also no difference for change in nODI from baseline to follow-up within NAWM or DAWM.

NDI. NAWM and DAWM had lower NDIs compared with HCWM (0.60 ± 0.05, 0.55 ± 0.05 versus 0.63 ± 0.02; $P < .05$, $P < .005$), and the NDI was lower in DAWM compared with NAWM (0.55 ± 0.05 versus 0.60 ± 0.05; $P < .05$) (Fig 1C).

Longitudinally, the NDI decreased by 4% ± 5% within NAWM from the enhancing-to-nonenhancing phase ($P < .005$; 2-sided paired *t* test). For lesion subgroups, NAWM NDI decreased by 6% ± 4% among the 9 subjects with any type 2 lesions (NDI decreasing lesions) ($P < .005$; 2-sided paired *t* test), whereas no significant NAWM NDI change was detectable among the 8 subjects without type 2 lesions (2% ± 5%, $P = .11$; 2-sided paired *t* test).

No significant longitudinal change was detected within DAWM in the transition from baseline to follow-up.

DTI Metrics. There was no difference in FA between NAWM and HCWM (Online Figure). DAWM showed lower FA compared with HCWM (0.45 ± 0.03 versus 0.48 ± 0.02; $P < .005$). NAWM and DAWM showed higher RD compared with HCWM ($440 \pm 25 \times 10^{-6}$, $474 \pm 37 \times 10^{-6}$ versus $0.426 \pm 14 \times 10^{-6}$; $P < .05$, $P < .005$). NAWM and DAWM, compared with HCWM, showed higher MD ($616 \pm 22 \times 10^{-6}$, $649 \pm 36 \times 10^{-6}$ versus $597 \pm 15 \times 10^{-6}$; $P < .005$) and AD ($961 \pm 28 \times 10^{-6}$, $996 \pm 39 \times 10^{-6}$ versus $934 \pm 26 \times 10^{-6}$; $P < .005$). Across time within the NAWM, there was an increase in RD ($440 \pm 25 \times 10^{-6}$ versus $448 \pm 33 \times 10^{-6}$; $P < .05$) and MD ($616 \pm 22 \times 10^{-6}$ versus $623 \pm 24 \times 10^{-6}$; $P < .005$).

DISCUSSION

Diffuse and focal WM microstructural changes were assessed across time in the transition from detectable to undetectable gadolinium enhancement. nODI values were consistently higher during the acute enhancing phase of a lesion compared with a later time point after resolution of enhancement (GELs versus GEL-FU) as well as within acute-versus-chronic lesions (GELs versus NGELs). The ODI might, therefore, represent a new potential marker of acute inflammation. Changes in NODDI parameters with time correlate with long-term evolution of lesion size.

nODI as a Marker of Acute Inflammation

Compared with HCs, markedly higher ODI values within MS lesions were observed during the acute inflammatory phase, indicated by gadolinium enhancement. These ODI values reduced toward HCWM values after the resolution of the enhancement. The association of higher ODI values with gadolinium enhancement suggests that ODI, when normalized for HC values (nODI), could be used as a potential radiologic marker of acute inflammation. The underlying histopathologic reasons for the nODI increase in the acute phase remain unknown.

A positive correlation between ODI and increased microglial density was reported in mice after withdrawal of colony-stimulating factor 1 receptor inhibition.[21] Likewise, the presence of a higher number of inflammatory cells within the core of acute-versus-chronic MS lesions[22] might partially explain the different ODI values detectable during gadolinium enhancement.

To date, only 1 longitudinal study assessed demyelinating lesions combining NODDI and histologic data. This work focused on a mouse model of toxic demyelination (injection of lysolecithin), characterized mainly by myelin content changes rather than inflammatory activity.[13] Most interesting, even in this model, focal lesions showed higher ODI values compared with healthy WM only at the peak of demyelination. These values, then, decreased with time to values similar to those in healthy WM.[13] This change suggests that the increased nODI within lesions in the acute phase might be connected not only with inflammatory changes but also the active demyelination detectable during gadolinium enhancement.[22]

Despite its possible association with inflammation, increased nODI is not unique to acute (gadolinium-enhancing) lesions but can sometimes also be detected in nonenhancing lesions. This finding may indicate that part of the pathophysiologic processes underlying an increase in nODI in the acute phase (ie, acute demyelination/inflammatory changes) might still be ongoing during the subacute phase, after blood-brain barrier closure. The fact that we detected decreasing nODI with time even within lesions that did not enhance at baseline (NGELs) indicates that nODI (and perhaps inflammation) keeps decreasing after enhancement resolution.

The existing NODDI literature on nonenhancing lesions is controversial. Our findings are consistent with the work of Granberg et al[10] comparing nonenhancing lesions with the contralateral NAWM. In contrast, a previous study found ODI to be lower in nonenhancing lesions than in HCWM.[7] This discrepancy might result from differences in location when comparing lesions. As a result of the dispersion and architectonic organization of the fibers, ODI varies across the normal brain, with lower values within main WM pathways (ie, corpus callosum, superior longitudinal fascicle) and higher values in the subcortical regions. We specifically addressed this issue in building a WM ODI atlas (see the Online Appendix for detailed technical description) to extract reference values for each lesion, thereby accounting for lesion location variability.

Only 1 study to date correlated NGEL ODI with pathology in subjects with MS. Specifically, Grussu et al[9] detected reduced ODI within chronic WM lesions confirmed by a histology-derived ODI, suggesting that neurites can have reduced orientation variability compared with healthy tissue within areas of focal demyelination and profound axonal loss. This finding is in contrast with our results, though differences in patient characteristics and anatomic sites investigated confound direct comparison of these studies.

Association of NDI and ODI Changes Over-Time as a Marker of Recovery and Possibly Remyelination

In line with previous cross-sectional studies,[7,10] we observed that NDI was consistently lower in WM lesions than in NAWM and HCWM. When we considered all GELs, NDI did not change during the transition from the acute-to-subacute phase, but at a single lesion level, we noticed a heterogeneity in the NDI changes with time. Approximately half (52%) of the lesions (type 1) showed increasing NDI over time along with decreasing ODI (Fig 2), whereas lesion type 2 (48% of the lesions) showed decreasing ODI and NDI with time (Fig 3).

In a toxic model of demyelination, remyelinating lesions showed a decreasing ODI and increasing NDI with time following the injury.[13] The authors suggested that these changes were

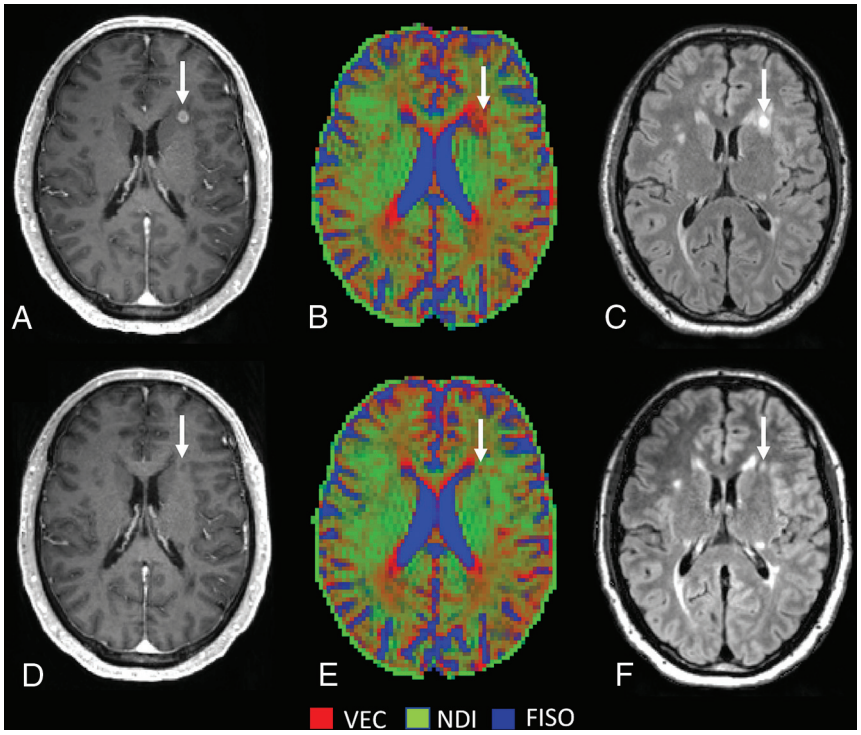

FIG 2. Lesion type 1 NODDI color map[8] graphically representing NDI (green) or VEC (red) compartment prevalence in voxels within a focal WM lesion (*white arrows*) at baseline (*A–C*) and at follow-up (after 12 months) (*D–F*). The green within the lesion is represented more at follow-up, after the disappearance of the enhancement, with a relative decrease of the red voxels. FLAIR sequences (*C* and *F*) show an important reduction in size with time. VEC and NDI are fractions in each voxel: If NDI increases, VEC decreases and vice versa. FISO indicates isotropic volume fraction.

due to increasing fiber coherency occurring along with the histologically-identified remyelination. With the precaution of translating these findings to MS, we speculate that the type 1 lesions we found might have a higher degree of remyelination compared with type 2 lesions, which might, in contrast, demonstrate ongoing tissue destruction. This hypothesis is supported by the finding that type 2 lesions also showed less shrinkage with time compared with type 1 lesions. Prior histopathologic data in MS suggest that remyelination occurs in approximately half of the lesions, a value similar in proportion to type 1 lesions in this study.[23]

NODDI Metrics in NAWM and DAWM

Even the longitudinal changes of NDI within the NAWM seem to depend on the predominant subtype of GEL. Specifically, subjects presenting exclusively with type 1 lesions did not show NDI changes with time within NAWM, whereas subjects with lesion type 2 (decreasing NDI with time, solely or combined with lesion type 1) showed decreasing NAWM NDI with time.

A report on scan-rescan reliability of NODDI showed that small biologic changes (<5%) may be detected with feasible sample sizes ($n < 6$–10).[24] The presence of type 2 lesions may, therefore, identify a subset of subjects characterized both by partial lack of focal remyelination and progressive ongoing NAWM damage. The latter may be a consequence of anterograde and retrograde degeneration secondary to axonal and neuronal damage within focal lesions.[25,26] In our study, only 3/17 participants showed exclusively type 2 lesions. Most interesting, 2 of them were the only primary-progressive cases included in the study, which might possibly indicate an association between type 2 lesions and a progressively worsening disease course.

Controversial results were reported for ODI changes within NAWM. We found lower ODI compared with HCWM, probably driven by predominant axonal loss rather than inflammation within NAWM.[27] In line with our findings, De Santis et al[12] found a trend for lower ODI in NAWM compared with HCWM, and a recent voxel-based-analysis study identified decreased ODI within the posterior and anterior limbs of the internal capsule with concomitant increased ODI in subcortical regions.[11] Another work, in contrast, found higher ODI in NAWM than in HCWM, possibly due to the limitations in ODI assessment as discussed above.[7] In the current study, we limited our analysis to the WM; therefore, our finding of slightly decreased ODI in NAWM might be mainly driven by changes in the major WM tracts.

Limitations

The present work shows several limitations: among them, the small number of subjects, the variable follow-up time, the absence of secondary-progressive MS participants, the convenience sampling, the lack of replication, and the possible confounding effect of various treatments.

Nonetheless, the lack of correlation with histopathologic data represents the most important limitation of our study. MR imaging/histopathology correlations are rarely performed in early relapsing-remitting MS due to limited tissue availability from biopsy, whereas postmortem studies mostly assess late disease stages. Our findings, however, are consistent with previous histologic studies. The higher ODI in the acute phase is likely to represent a combined result of inflammatory changes[21] and demyelination.[13] Regarding changes with time, our results are comparable with the only longitudinal work correlating NODDI metrics with histopathologic changes within focal demyelinated plaques.[13] The current work, however, only suggests speculative hypotheses that should be further confirmed with histopathologic correlation studies.

An additional important limitation of this work is that NDI does not represent an absolute but rather represents a relative measurement of neurite density. NODDI models the relative contribution of the intraneurite compartment (NDI) to the total diffusion signal in each voxel. Within brain tissue voxels, this compartment is mainly distinguished from the extra-neurite compartment (VEC), whereas the purely isotropic contribution does not play a major role. An increase in NDI might, therefore, indicate either a higher density of neurites or a reduced contribution by extracellular

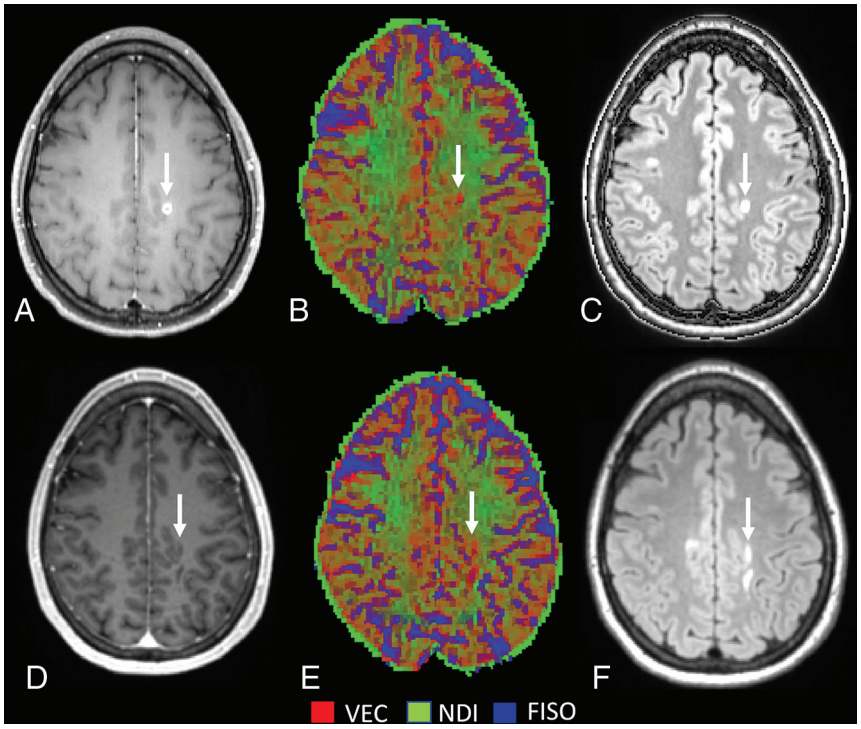

FIG 3. Lesion type 2 NODDI color map[8] graphically representing NDI (green) or VEC (red) compartment prevalence in voxels within a focal WM lesion (*white arrows*) at baseline (*A–C*) and at follow-up (after 15 months) (*D–F*). The green within the lesion is less represented at follow-up after the disappearance of the enhancement, with a relative increase of the red voxels. FLAIR sequences (*C* and *F*) show a moderate reduction in size with time. VEC and NDI are fractions in each voxel: If NDI decreases, VEC increases and vice versa. FISO indicates isotropic volume fraction.

spaces or other cell types. An increase in NDI with time is, indeed, theoretically consistent with both remyelination (NDI increases indicating recovery of axonal integrity) and reduction of inflammation (VEC decreases associated with reduction of edema and inflammatory cells).

CONCLUSIONS

NODDI-derived metrics showed an intriguing potential in detecting acute inflammation and ongoing inflammatory disease activity. Assessing their changes with time might permit categorization of subacute and chronic lesion evolution in MS. The consistency of our MR imaging findings in subjects with MS with previous findings in animal models and the histopathologic correlation between NDI/ODI changes with time with remyelination suggest that NODDI imaging is also a potential tool to assess responses to neuroprotective or remyelinating therapies in vivo.

Disclosures: Simone Sacco—*UNRELATED*: *Employment*: University of Pavia, Italy, University of California, San Francisco. Riley M. Bove—*UNRELATED*: *Comments*: research; *Provision of Writing Assistance, Medicines, Equipment, or Administrative Support*: Genzyme Sanofi, *Comments*: writing assistance; *Consultancy*: Alexion, Biogen, EMD Serono, Roche Genentech, Genzyme Sanofi, Novartis; *Grants/Grants Pending*: Akili Interactive.* Jeffrey M. Gelfand—*UNRELATED*: *Consultancy*: Biogen, Alexion Pharmaceuticals; *Grants/Grants Pending*: Genentech, *Comments*: research support for a clinical trial.* Douglas S. Goodin—*UNRELATED*: *Board Membership*: Biogen Idec, Bayer Schering Pharma, Novartis, EMD Serono, Genzyme, and Teva Pharmaceuticals; *Consultancy*: Biogen Idec, Bayer Schering Pharma, Novartis, EMD Serono, Genzyme, and Teva Pharmaceuticals; *Employment*: Biogen Idec, Bayer Schering Pharma, Novartis, EMD Serono, Genzyme, and Teva Pharmaceuticals; *Grants/Grants Pending*: Biogen Idec, Bayer Schering Pharma, Novartis, EMD Serono, Genzyme, and Teva Pharmaceuticals; *Payment for Lectures Including Service on Speakers Bureaus*: Biogen Idec, Bayer Schering Pharma, Novartis, EMD Serono, Genzyme, and Teva Pharmaceuticals. Roland G. Henry—*RELATED*: *Grant*: Roche/Genentech, Atara Biotherapeutics; *Consulting Fee or Honorarium*: Roche/Genentech, Novartis, Sanofi/Genzyme, QIA Consulting; *UNRELATED*: *Board Membership*: AbbVie, Roche, and Novartis; *Employment*: UCSF; *Expert Testimony*: StemCells Inc, Hoffmann-La Roche, and Sanofi Genzyme*; *Grants/Grants Pending*: Ari J. Green—*UNRELATED*: *Board Membership*: Biogen and Medimmune, Novartis and Scientific Advisory Board for Bionure; *Consultancy*: Inception Sciences and Mylan Pharmaceuticals; *Employment*: UCSF; *Grants/Grants Pending*: National MS Society, Novartis, University of California San Francisco, CTSI, That Man May See. Bruce A. Cree—*UNRELATED*: *Consultancy*: Akili INteractive, Alexion, Atara Biotherapeutics, Biogen, EMD Serono, Novartis, Sanofi, and TG Therapeutics. Stephen L. Hauser—*RELATED*: *Grant*: National Institutes of Health/National Institute of Neurological Disorders and Stroke, National MS Society, Valhalla Charitable Foundation, *Comments*: R35NS111644, RR 2005-A-13; *UNRELATED*: Dr Hauser serves on the Board of Directors and received stock options for Neurona Therapeutics and serves on the Scientific Advisory Board and received stock options for Accure, Alector, Annexon Biosciences, and Molecular Stethoscope; he has also received nonfinancial support from Hoffmann-La Roche and Novartis (travel reimbursement and writing support for anti-CD20 meetings and presentations). Michael R. Wilson—*UNRELATED*: *Grants/Grants Pending*: Roche/Genentech.* Scott S. Zamvil—*UNRELATED*: *Board Membership*: Deputy Editor, *Neurology*, *Neuroimmunology and Neuroinflammation*; *Consultancy*: Alexion, Biogen Idec, Genzyme, Novartis, Roche/Genentech, Teva Pharmaceuticals; *Grants/Grants Pending*: National Institutes of Health 1 R01 AI13624-01-A1, National Institutes of Health R21 NS1081590-01, 1R21 AI142186-01*; *Payment for Lectures Including Service on Speakers Bureaus*: Alexion, Genzyme, Novartis.*Money paid to the institution.

REFERENCES

1. Thompson AJ, Banwell BL, Barkhof F, et al. **Diagnosis of multiple sclerosis: 2017 revisions of the McDonald criteria.** *Lancet Neurol* 2018;17:162–73 CrossRef Medline
2. Filippi M, Rocca MA, Ciccarelli O, et al. **MRI criteria for the diagnosis of multiple sclerosis: MAGNIMS consensus guidelines.** *Lancet Neurol* 2016;15:292–303 CrossRef
3. De Groot CJ, Bergers E, Kamphorst W, et al. **Post-mortem MRI-guided sampling of multiple sclerosis brain lesions: increased yield of active demyelinating and (p)reactive lesions.** *Brain* 2001;124:1635–45 CrossRef Medline
4. Cercignani M, Bozzali M, Iannucci G, et al. **Intra-voxel and inter-voxel coherence in patients with multiple sclerosis assessed using diffusion tensor MRI.** *J Neurol* 2002;249:875–83 CrossRef Medline
5. Gulani V, Calamante F, Shellock FG, et al; International Society for Magnetic Resonance in Medicine. **Gadolinium deposition in the brain: summary of evidence and recommendations.** *Lancet Neurol* 2017;16:564–70 CrossRef Medline
6. Zhang H, Schneider T, Wheeler-Kingshott CA, et al. **NODDI: practical in vivo neurite orientation dispersion and density imaging of the human brain.** *Neuroimage* 2012;61:1000–16 CrossRef Medline

7. Schneider T, Brownlee W, Zhang H, et al. **Sensitivity of multi-shell NODDI to multiple sclerosis white matter changes: a pilot study.** *Funct Neurol* 2017;32:97–101 CrossRef Medline
8. Caverzasi E, Papinutto N, Castellano A, et al. **Neurite orientation dispersion and density imaging color maps to characterize brain diffusion in neurologic disorders.** *J Neuroimaging* 2016;26:494–98 CrossRef Medline
9. Grussu F, Schneider T, Tur C, et al. **Neurite dispersion: a new marker of multiple sclerosis spinal cord pathology?** *Ann Clin Transl Neurol* 2017;4:663–79 CrossRef Medline
10. Granberg T, Fan Q, Treaba CA, et al. **In vivo characterization of cortical and white matter neuroaxonal pathology in early multiple sclerosis.** *Brain* 2017;140:2912–26 CrossRef Medline
11. Spanò B, Giulietti G, Pisani V, et al. **Disruption of neurite morphology parallels MS progression.** *Neurol Neuroimmunol Neuroinflamm* 2018;5:e502 CrossRef Medline
12. De Santis S, Bastiani M, Droby A, et al. **Characterizing microstructural tissue properties in multiple sclerosis with diffusion MRI at 7T and 3T: the impact of the experimental design.** *Neuroscience* 2019;403:17–26 CrossRef Medline
13. Luo T, Oladosu O, Rawji KS, et al. **Characterizing structural changes with devolving remyelination following experimental demyelination using high angular resolution diffusion MRI and texture analysis.** *J Magn Reson Imaging* 2019;49:1750–59 CrossRef Medline
14. University of California, San Francisco MS-EPIC Team, Cree BA, Gourraud PA, et al. **Long-term evolution of multiple sclerosis disability in the treatment era.** *Ann Neurol* 2016;80:499–510
15. University of California, San Francisco MS-EPIC Team, Cree BAC, Hollenbach JA, et al. **Silent progression in disease activity-free relapsing multiple sclerosis.** *Ann Neurol* 2019;85:653–66
16. Andersson JL, Skare S, Ashburner J. **How to correct susceptibility distortions in spin-echo echo-planar images: application to diffusion tensor imaging.** *Neuroimage* 2003;20:870–88 CrossRef Medline
17. Smith SM, Jenkinson M, Woolrich MW, et al. **Advances in functional and structural MR image analysis and implementation as FSL.** *Neuroimage* 2004;23(Suppl 1):S208–19 CrossRef Medline
18. Garyfallidis E, Brett M, Amirbekian B, et al; DIPY Contributors. **DIPY, a library for the analysis of diffusion MRI data.** *Front Neuroinform* 2014;8:8 CrossRef Medline
19. Moore GR, Laule C, Mackay A, et al. **Dirty-appearing white matter in multiple sclerosis: preliminary observations of myelin phospholipid and axonal loss.** *J Neurol* 2008;255:1802–11 CrossRef Medline
20. Smith SM, Zhang Y, Jenkinson M, et al. **Accurate, robust and automated longitudinal and cross-sectional brain change analysis.** *Neuroimage* 2002;17:479–49 CrossRef Medline
21. Yi SY, Barnett BR, Torres-Velázquez M, et al. **Detecting microglial density with quantitative multi-compartment diffusion MRI.** *Front Neurosci* 2019;13:81 CrossRef Medline
22. Popescu BF, Pirko I, Lucchinetti CF. **Pathology of multiple sclerosis: where do we stand?** *Continuum (Minneap Minn)* 2013;19:901–21 CrossRef Medline
23. Barkhof F, Brück W, De Groot CJ, et al. **Remyelinated lesions in multiple sclerosis: magnetic resonance image appearance.** *Arch Neurol* 2003;60:1073–81 CrossRef Medline
24. McCunn P, Gilbert KM, Zeman P, et al. **Reproducibility of neurite orientation dispersion and density imaging (NODDI) in rats at 9.4 Tesla.** *PLoS One* 2019;14:e0215974 CrossRef Medline
25. Lassmann H. **Multiple sclerosis pathology.** *Cold Spring Harb Perspect Med* 2018;8:a028936 CrossRef Medline
26. Haider L, Zrzavy T, Hametner S, et al. **The topography of demyelination and neurodegeneration in the multiple sclerosis brain.** *Brain* 2016;139:807–15 CrossRef Medline
27. Thompson AJ, Baranzini SE, Geurts J, et al. **Multiple sclerosis.** *Lancet* 2018;391:1622–36 CrossRef Medline